

References

- 1 Li, H. M., Developing trend of gear, chain, and belt, *Mechanical Transmission* (in Chinese), 1992, 16(1): 1.
- 2 Tang, D. G., Chen, G. M., The current situation and forecast of gear transmission technology, *Journal of Mechanical Engineering* (in Chinese), 1993, 29(5): 35.
- 3 Khrama, A., Singh, R., Interactions between time-varying mesh stiffness and clearance non-linearities in a geared system, *J. of Sound and Vibration*, 1991, 146(1): 135.
- 4 Ozguven, H. N., Houser, D. R., Dynamic analysis of high speed gears by using loaded static transmission error, *J. of Sound and Vibration*, 1988, 125(1): 71.
- 5 Kasuba, R., Evans, J. W., An extended model for determining dynamic loads in spur gearing, ASME, *J. of Mech. Des.*, 1981, 103: 399.
- 6 Wang, S. Y., Determination of δ and C of gear tooth deformation, *Journal of Shandong University of Technology* (in Chinese), 1981, 11(4): 45.
- 7 Hugo, D. N., Guillermo, H. K., Automatic digital processing in speckle photography: comparison of two algorithms, *Appl. Opt.*, 1989, 28(2): 350.
- 8 Vest, C. M., *Holographic Interferometry*, New York: John Wiley & Sons, 1979, 52.
- 9 Li, J. F., Gao, Q., Tian Z. R., et al., Approach to eliminate the influence of diffraction halo in speckle photographic fringe, *AMSE, Advances in Modelling & Analysis, B*, 1995, 34(1): 19.
- 10 Li, J. F., Study of gear tooth instantaneous stiffness, *Dissertation*, Jinan: Shandong University of Technology, 1994.

(Received August 6, 1997)

Point defects in active layers of TFEL devices based on ZnS

LOU Zhidong¹, A. N. Georgobiani², XU Zheng³, XU Chunxiang⁴,
TENG Feng⁴, YU Lei⁴ and XU Xurong^{3,5}

1. Applied Physics Department, Tianjin University, Tianjin 300072, China; 2. P. N. Lebedev Physical Institute, Russian Academy of Sciences, 117924 Moscow, Russian; 3. Physics Department, Northern Jiaotong University, Beijing 100044, China; 4. Institute of Material Physics, Tianjin Institute of Technology, Tianjin 300191, China; 5. Laboratory of Excited State Processes, Changchun Institute of Physics, Chinese Academy of Sciences, Changchun 130021, China

Abstract Point defects in the active layer of a layered optimization thin film electroluminescent device of ZnS:Er³⁺ were studied. The results indicate that besides Er³⁺ substituting for Zn²⁺ as luminescent centers, the dominant point defects are sulfur vacancies, zinc vacancies, shallow donors and deep acceptors. Their influence on electroluminescence is discussed.

Keywords: spectra of photoluminescence, point defects, thin film electroluminescence.

THE outstanding issue in the field of thin film electroluminescence (TFEL) is how to improve the blue brightness. Zinc sulfide (ZnS) is an important commercial TFEL material. Rare earth such as Er, Ce and Tb are usually doped into ZnS to obtain green or blue TFEL. The mechanism of electroluminescence indicates that the dominant factor affecting blue emission is hot electron energy. Xu *et al.*^[1,2] put forward the structure of the layered optimization TFEL in order to solve this problem. According to his structure, the region of excitation of luminescent centers is separated from that of acceleration of hot electrons, and SiO₂ is used as the accelerating layer. It has been proved by some experiments that a large proportion of the intensity of the short wavelength emission can be achieved with this structure.

There exist many point defects in the active layers of TFEL devices due to some inevitable physical and chemical factors during thin film depositing, which influence the properties of electroluminescence. The dominant point defects in the active layers of TFEL devices based on ZnS are vacancies and impurities^[3]. In the present note the influence of the point defects in ZnS:Er³⁺ on TFEL is discussed.

1 Sample preparation

There are two kinds of samples: powder ZnS:Er³⁺ in the form of pellet and thin film ZnS:Er³⁺. A small amount of NH₄Cl was doped into pure powder ZnS or powder ZnS with 0.5 mol% ErF₃ as flux. After the mixture was ground completely, pellets for deposition were formed by a compressor. Then the pellets were baked for 1.5 h at 1100 °C. Thin film samples were prepared with the electron beam evapora-

tion method.

2 Experimental results and discussion

According to the method of sample preparation, there may exist the following point defects in ZnS: Er³⁺: substitutional anions Er_{Zn}, Cl⁻¹ and F⁻¹, sulfur vacancies V_S, zinc vacancies V_{Zn} and a small amount of other uncontrollable impurities.

2.1 Substitutional anion Er_{Zn}

Rare earth ions on zinc sites in ZnS normally act as luminescent centers, such as Er_{Zn}. They are discrete luminescent centers which have almost the same energy level structures as free ones. Fig. 1 is the electroluminescent spectrum of a ZnS: Er³⁺ TFEL device arising from the dipole transitions between 4f energy levels. The main peaks are located at 528.5 nm and 549.5 nm corresponding to the ²H_{11/2} → ⁴I_{15/2} and ⁴S_{3/2} → ⁴I_{15/2} transitions, respectively. Usually the intensity of the former is stronger than the latter. There is also a red peak located at 665.0 nm corresponding to ⁴F_{9/2} → ⁴I_{15/2}. Besides, there are some weaker blue peaks.

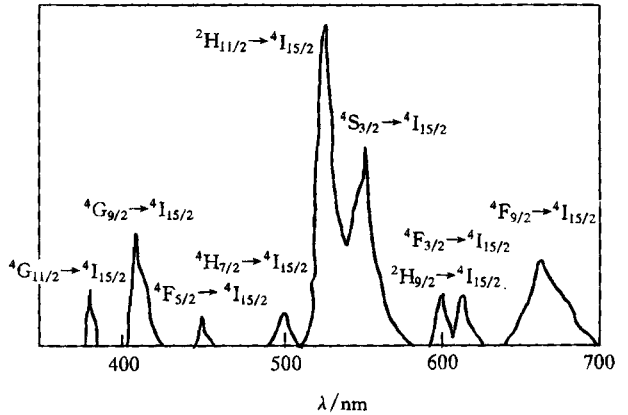


Fig. 1. EL spectrum of ZnS: Er³⁺.

We can draw a conclusion that Er³⁺ ions are mainly introduced into ZnS lattice during evaporation deposition from the photoluminescent spectra of powder ZnS:Er³⁺, ZnS(Cl) and thin film ZnS:Er³⁺ at room temperature (figs. 2 and 3) under excitation of N₂ laser (337.1 nm, 3 × 10⁻⁸ s). In powder ZnS:Er³⁺, there only exists the same blue band centered at 449.0 nm as powder ZnS(Cl), but no emitting peaks of Er³⁺ exist. This blue band is a typical self-activated emitting band which is attributable to zinc vacancies^[4]. We observed three sets of peaks of Er³⁺ in about 4-μm-thick thin film ZnS:Er³⁺. These peaks are added to a very wide background band which may be caused by dust. The first set of peaks due to the ⁴F_{7/2} → ⁴I_{15/2} transition are located at 485.1, 491.6 and 494.8 nm, respectively. The second set due to ²H_{11/2} → ⁴I_{15/2} are centered at 518.0, 522.4 and 527.3 nm, respectively. The third due to ⁴S_{3/2} → ⁴I_{15/2} are located at 559.7, 564.5 and 567.8 nm, respectively. There are three peaks corresponding to every transition, which indicates that the energy levels of Er³⁺ are split by the crystal field. This phenomenon cannot be observed in electroluminescence. Perhaps it is the electric field

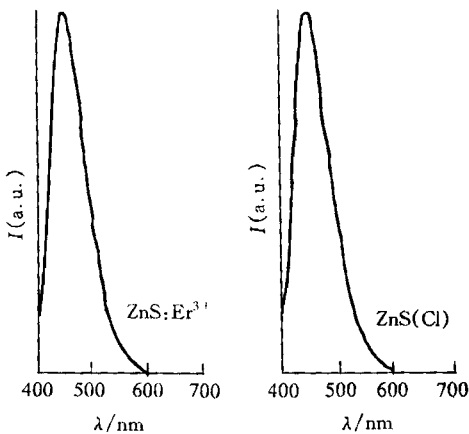


Fig. 2. PL spectra of powder ZnS: Er³⁺ and ZnS(Cl).

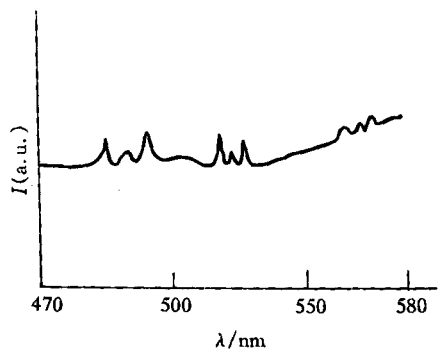


Fig. 3. PL spectrum of thin film ZnS: Er³⁺.

that offsets the influence of the crystal field.

There are two factors responsible for no light emitting of Er^{3+} in powder $\text{ZnS}:\text{Er}^{3+}$. First, there are few Er^{3+} ions that can enter powder ZnS lattice. Even if there are some, their light emission are very weak and covered by the strong recombination emission of ZnS . Second, the distribution of Er^{3+} ions in powder $\text{ZnS}:\text{Er}^{3+}$ is not uniform since they are introduced into ZnS by the method of solid state mixing. It is possible that concentration quenching of Er^{3+} occurs, for some Er^{3+} clusters form on the surface of ZnS . However, the Er^{3+} clusters are broken up during the preparation of thin film $\text{ZnS}:\text{Er}^{3+}$, and the distribution of Er^{3+} ions becomes uniform. Therefore, Er^{3+} ions are introduced into the lattice during evaporation deposition.

2.2 Vacancies

Figure 4 illustrates the photoluminescent spectrum of thin film $\text{ZnS}(\text{Cl})$ under N_2 laser excitation. There is a blue band centered at 463.9 nm and a green shoulder centered at 524.6 nm at both room temperature and 77 K, but the intensities at 77K are higher. They are self-activated recombination luminescence of ZnS attributable to the intrinsic defects in ZnS . Georgobiani^[4] attributed the blue band to zinc vacancies, which comes from the transition of electrons from the conduction band to the singly-charged zinc vacancies $\text{V}_{\text{Zn}}^{1-}$. From the maximum position of the blue band in fig. 4, the optical activation energy of $\text{V}_{\text{Zn}}^{1-}$ was calculated to be at about 2.67 eV below the conduction band minimum, and 1.00 eV above the valence band maximum (the width of the forbidden band of ZnS is about 3.70 eV). The self-activated green shoulder relates to sulfur vacancies, which arises from the transition of electrons from the conduction band to the doubly-charged sulfur vacancies V_{S}^{2+} . V_{S}^{2+} was calculated to be at 2.36 eV below the conduction band minimum. Deng^[5] indicated that there is a deep level at 2.14 eV below the conduction band minimum, which is very close to our estimation of V_{S}^{2+} . Besides, our estimation of V_{S}^{2+} approaches Pecheur's theoretical value^[6] (at 2.48 eV below the conduction band) very much.

From fig. 3 we know that photoluminescence in thin film $\text{ZnS}:\text{Er}^{3+}$ is mainly the emission of Er^{3+} ions. There are not any self-activated blue band and green shoulder of ZnS because the electron energy in the conduction band is transferred to the excited energy levels of Er^{3+} . However, there also exist S vacancies and Zn vacancies in thin film $\text{ZnS}:\text{Er}^{3+}$ due to self-compensation.

(1) Sulfur vacancies V_{S} . A sulfur vacancy is a double donor^[3] which has two levels in the forbidden band of ZnS . One is a singly-charged S vacancy V_{S}^{1+} , and the other is a doubly-charged S vacancy V_{S}^{2+} . Simple electrostatic repulsive energy considerations suggest that the separation between the first and second ionization of V_{S} is normally 1.00 eV^[7]. We have already known that V_{S}^{2+} is at about 2.36 eV below the conduction band maximum, therefore V_{S}^{1+} is at about 1.36 eV below the conduction band maximum, which approaches Madelung's estimation of V_{S}^{1+} (at 1.4 eV below the conduction band maximum)^[8] very much. There are two factors responsible for the generation of sulfur vacancies. First, in order to get thin film with good crystallinity, the substrate temperature is always kept at 250°C or so. S ions would rapidly reevaporate from the hot substrate due to the high vapor pressure. Secondly, S vacancies may be considered as a consequence of the self-compensation of some uncontrollable shallow acceptors.

The Auger type-nonradiative energy transfer via sulfur vacancies^[9,10] occurs in $\text{ZnS}:\text{Ce}^{3+}$ and $\text{ZnS}:\text{Tb}^{3+}$ TFEL devices. This model is suitable to $\text{ZnS}:\text{Er}^{3+}$, too. The relative intensities of Er^{3+} peaks mainly depend on the impact excitation cross-sections, life times and state densities of Er^{3+} energy levels,

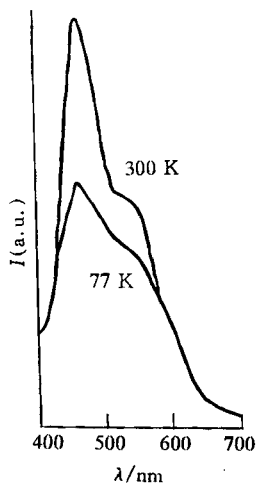


Fig. 4. PL spectra of thin film $\text{ZnS}(\text{Cl})$.

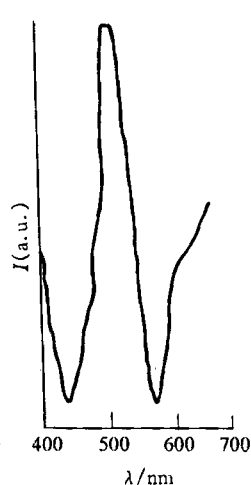


Fig. 5. PL spectrum of Cu^{3+} in powder $\text{Zn}(\text{Cl})$.

and are also affected by the nonradiative energy transfer via sulfur vacancies. We have already known that the two levels V_S^{1+} and V_S^{2+} of S vacancies are located at 1.36 and 2.36 eV below the conduction band maximum. V_S^{1+} is known to have a strong Gaussian absorption F band centered at 2.27 eV and a weaker asymmetric absorption K band at 2.88 eV^[11]. V_S^{2+} captures an electron from the conduction band or the surrounding Zn^{2+} ions initially and becomes V_S^{1+} . A part of the dipole ${}^2H_{11/2} \rightarrow {}^4I_{15/2}$ (528.5 nm, 2.35 eV) and ${}^4S_{3/2} \rightarrow {}^4I_{15/2}$ (549.5 nm, 2.26 eV) transition energies is transferred to the absorption F band of V_S^{1+} centered at 2.27 eV. The probability of the energy transfer is proportional to the spectral overlapping between the emission and the absorption, and is in inverse proportion to the sixth power of the distance between Er^{3+} and V_S . Therefore, the ${}^4S_{3/2} \rightarrow {}^4I_{15/2}$ transition transfers more energy to the F band of V_S^{1+} than the ${}^2H_{11/2} \rightarrow {}^4I_{15/2}$. This may be one of the reasons why the intensity of the ${}^4S_{3/2} \rightarrow {}^4I_{15/2}$ transition is weaker. The emitting intensities of the ${}^4F_{5/2} \rightarrow {}^4I_{15/2}$ (458.0 nm, 2.71 eV) and ${}^4F_{7/2} \rightarrow {}^4I_{15/2}$ (494.0 nm, 2.51 eV) transitions are lowered to a certain extent by the nonradiative energy transfer via V_S^{1+} .

So long as sulfur vacancies exist in the active layer of a ZnS TFEL device, it is inevitable that a part of the transition energy of short wavelength (blue or green) is lost. However, the luminance of short wavelength could be increased by restricting the amount of sulfur vacancies. Our study of $ZnS_xO_{1-x}: Ce^{3+}$ TFEL devices^[12] indicated that when oxygen substitutes for sulfur vacancies, the nonradiative energy transfer via V_S^{1+} is prevented, and the luminance of Ce^{3+} increases by about ten times.

(2) Zinc vacancies V_{Zn} . A zinc vacancy is a double acceptor with two states in the forbidden band: singly-charged Zn vacancy V_{Zn}^{1-} and doubly-charged Zn vacancy V_{Zn}^{2-} . V_{Zn}^{1-} in ZnS: Er^{3+} thin film has been estimated to be at 2.67 eV below the conduction band maximum or 1.00 eV above the valence band minimum, which exactly equals the value of V_{Zn}^{1-} Douglas^[13] estimated. V_{Zn}^{2-} was roughly investigated to be at 1.50 eV above the valence band maximum^[7]. Zn vacancies caused by the self-compensation of Cl and F could influence thin film electroluminescence. Douglas *et al.*^[13] and Shih *et al.*^[14] attributed the origin of space charge to impact ionization of zinc vacancies. Losing an electron, V_{Zn}^{2-} becomes V_{Zn}^{1-} . There are two advantages of space charge generation: improving aging stability and reducing threshold voltage.

3 Shallow donors and some other uncontrollable anion impurities

Cl^{-1} ions were introduced into ZnS because of flux NH_4Cl . The ionic radii of Cl^{-1} and S^{2-} are 0.181 and 0.184 nm, respectively. The close size match of Cl and S suggests that Cl will invariably be incorporated as a substitutional donor Cl_S . Er^{3+} ions were introduced into ZnS in the form of a fluoride. The ionic radius of F^{-1} is 0.136 nm, much smaller than that of S^{2-} . Electro-negative ions F^{-1} also act as substitutional donors F_S . Shallow donors Cl_S and F_S with their level depths being several tenth eV are electron traps. Space charge can be generated by their field emission at electric fields.

Some anion impurities could be introduced into ZnS inadvertently. We observed the photoluminescence of Cu^+ in powder ZnS. Fig. 5 is its spectrum under xenon lamp (369 nm) as an excitation source. We found a green band centered at 510 nm which had afterglow after the xenon lamp was turned off, suggesting that this would be the luminescence of Cu^+ . Cu^+ substituting for Zn^{2+} is a deep level at 1.26 eV above the valence band maximum. The influence of Cu^+ remains to be solved.

4 Conclusions

In this note we studied the energy level positions in the forbidden band of the point defects in ZnS: Er^{3+} thin film with the photoluminescence measurements. The results indicate that besides Er^{3+} substituting for Zn^{2+} as luminescent centers, the dominant point defects are sulfur vacancies, zinc vacancies, shallow donors Cl_S and F_S , deep acceptors Cu^+ and some other uncontrollable shallow acceptors. Zinc vacancies are a double acceptor and sulfur vacancies are a double donor. According to our investigations, V_S^{1+} and V_S^{2+} are at 1.36 and 2.36 below the conduction band minimum, respectively; V_{Zn}^{1-} and V_{Zn}^{2-} are at 1.00 eV and 1.50 eV above the valence band, respectively; and Cu^+ is at 1.26 eV above the valence band.

In the meantime we discussed the influence of the above-mentioned point defects on electrolumi-

nescence. The blue and green emission of Er^{3+} is decreased due to the Auger type-nonradiative energy transfer via sulfur vacancies. Space charge generation occurs through the field emission of Cl_S and F_S and the impact ionization of V_{Zn}^{2-} .

Acknowledgement This work was supported by the National Natural Science Foundation of China (Grant No. 19334030), and is a joint project in the framework of cooperation between Chinese Foundation of Natural Sciences and Russian Foundation of basic research. The photoluminescent experiments were finished in Vavilov Laboratory of Luminescence, P. N. Lebedev Physical Institute, Russian Academy of Sciences.

References

- 1 Xu, X. R., Lei, G., Shen, M. Y., Trial for electroluminescence of the third generation, *Advance in Natural Sciences*, 1991, 1: 62.
- 2 Lei, G., Xu, Z., Xu, X. R., An EL devices of spatial separation of carrier acceleration and excitation, *Journal of Luminescence* 1991, 48&49: 881.
- 3 Wager, J. F., Electroluminescent phosphors: point defect, in *Proceedings of 1996 International Workshop on Electroluminescence*, Berlin: Wissenschaft & Technik Verlag, 1996, 33.
- 4 Georgobiani, A. N., Lepnev, L. S., Panasyuk, Y. I. *et al.* Infrared photoluminescence of zinc sulfide, in *Proceedings of the Labedev Physics Institute, Academy of Sciences of the USSR*, 1988, 182: 1.
- 5 Deng, Z. B., Chen, L. C., Gao, Y. *et al.*, Deep levels of thin film electroluminescent devices, in *Proceedings of 1994 International Workshop on Electroluminescence*, Beijing: Science Press, 1994, 332.
- 6 Pecheur, P., Kauffer, E., Gerl, M., Tight-binding calculation of the properties of the F center and of isoelectronic defects in ZnS, *Phys. Rev.*, 1976, B14: 4521.
- 7 Kroger, F. A., *The Chemistry of Imperfect Crystals*, 2nd ed., Amsterdam: North-Holland, 1974, 2.
- 8 Madelung, O., Ed. *Landolt-Bornstein*, new series, Berlin: Springer-Verlag, 1982, 17b: 61.
- 9 Sohn, S. H., Yoshihiro Hamakawa, A model for emission from ZnS:Ce³⁺ and SrS:Ce³⁺ thin-film electroluminescent devices. *Jpn. J. Appl. Phys.*, 1992, 31: 3901.
- 10 Sohn, S. H., Hyun, D. G., Noma, M. *et al.* Effects of oxygen on electroluminescent characteristics of ZnS: TbOF and ZnS: TmOF devices, *J. Appl. Phys.*, 1992, 72(10): 4877.
- 11 Schneider, P., II - VI *Semiconducting Compounds* (ed. Thomas, D. G.), New York: Benjamin, 1967, 1.
- 12 Yu, L., Lou, Z. D., Xu, C. X., The new trial for raising brightness of blue-green TFEL device, in *Proceedings of 1996 International Workshop on Electroluminescence*, Berlin: Wissenschaft & Technik Verlag, 1996, 307.
- 13 Douglas, A. A., Wager, J. F., Evidence for space charge in atomic layer epitaxy ZnS:Mn alternating-current thin-film electroluminescent devices, *J. Appl. Phys.*, 1993, 73(1): 296.
- 14 Shih, S., Keir, P. D., Wager, J. F., Space charge generation in ZnS: Mn alternating-current thin-film electroluminescent devices. *J. Appl. Phys.*, 1995, 78(9): 5775.

(Received September 5, 1997)

Identification of a DNase activated in *Xenopus* egg extracts undergoing apoptosis

ZHU Shan, JIANG Zhengfan, ZHANG Bo, LU Zhigang
and ZHAI Zhonghe*

College of Life Sciences, Peking University, Beijing 100871, China. * Corresponding author, E-mail address: swzb@ibmstone.pku.edu.cn.

Abstract A cell-free apoptosis system was established by adding dATP and cytochrome c to *Xenopus laevis* egg extracts S-150. Accompanied by an incubation process, an apoptosis-specific DNase was activated in egg extracts which depended on Mg^{2+} and inhibited by Zn^{2+} . Two nucleases existing in egg extracts were revealed by in-gel nuclease assay. Further experiments showed that 27 ku nuclease which was different from other $\text{Ca}^{2+}/\text{Mg}^{2+}$ -dependent nucleases was a possible candidate involved in apoptosis.

Keywords: apoptosis, DNase, cell-free system, *Xenopus* egg extracts.

APOPTOSIS is a mode of cell death characterized by distinct morphological features, such as membrane blebbing, cytoplasmic and nuclear condensation, chromatin aggregation and formation of apoptotic bodies^[1]. Multiple evidence shows that the activation of cystine protease interleukin 1 β converting-enzyme